SAE INTERNATIONAL

ARTICLE INFO
Article ID: 05-11-03-0017

doi:10.4271/05-11-03-0017

Data Manipulation Approach and Parameters Interrelationships of the High-Pressure Torsion for AA6061-15%SiC_p Composite

Waleed El-Garaihy, *Suez Canal University and Qassim University*
El-sayed Abd El Rassoul, *Mansoura University*
Abdulrahman Al Ateyah, *Qassim University*
Ayman Mohamed Alaskari, *PAAET*
Samy Oraby, *PAAET*

Abstract

On contrast to the qualitative approach used in the majority of researches, an evaluation quantitative approach is introduced not only to depict the plain individual effect of the influence of the high-pressure torsion (HPT) processing conditions on the microstructural and Hv-values of the ultra-hard nanostructured AA6061-15%SiCp composite but also to detect its possible parameters functional interaction and nonlinear trends involved. Experimental data were used to establish many adequate and significant empirical models to detect and to evaluate the mutual functional interrelationships between the Hv-values of the composite, each of HPT processing pressure, and number of revolutions. For each group of interrelated parameters, the preferred selected developed model has been exploited to generate the relevant contours and response surface graphs. On one hand, it is shown that HPT processing can be improved through applying the best effective methods to produce materials with a nanostructure, while maintaining higher durability; in addition to a superior hardness. On the other hand, the development of functional outcome in mathematical forms becomes an essential requirement in nowadays digital database era.

History

Received: 11 Aug 2017
Revised: 11 Dec 2017
Accepted: 30 Jan 2018
e-Available: 29 May 2018

Keywords

Response surface methodology, non-linear regression procedures, high-pressure torsion (HPT), AA6061-SiC composite, severe plastic deformation

Citation

El-Garaihy, W., El Rassoul, E.A., Al Ateyah, A., Alaskari, A.M. et al., "Data Manipulation Approach and Parameters Interrelationships of the High-Pressure Torsion for AA6061-15%SiC_p Composite," *SAE Int. J. Mater. Manuf.* 11(3):2018, doi:10.4271/05-11-03-0017.

ISSN: 1946-3979
e-ISSN: 1946-3987

Introduction

Aluminum matrix composites (AMCs) reinforced with nonmaterial is a specific type of materials which is based on a minimum of two distinctive phases of physical and chemical characteristics. Such a type is a rapidly rising branch of materials science especially with the emergence of powder-based additive manufacturing methods [1, 2, 3]. These material systems revealed effectiveness in obtaining ameliorated properties of materials, which led to an obvious attraction to scientists working in materials area [4]. However, some design drawbacks still to be resolved including the little interfacial bonding taking place through the reinforcement and the Al matrix, in addition to the disadvantages accompanied by having weak dispersion and low stability of reinforcement in Al composites [5, 6, 7].

Since its use for manufacturing, the AMCs, powder metallurgy (PM) technique proved merit to produce controlled properties of materials through an accurate manipulation of the microstructure. Reaching ameliorated composites' mechanical properties is attainable via precise homogenization, which allows reinforcement particles distributed evenly within the composite matrix [8]. Very high strains are the most essential requirements for the enhancement process of homogeneity, particularly when dealing with composites having fine particles [9]. As a result, many researchers [4, 10, 11] tended to use the severe plastic deformation (SPD) process, owing to its high potential of particle distribution homogeneity amelioration, and to its great efficiency in Al alloys grain refinement to ultra-fine scale, as well as to its tendency to decrease impurities and residual porosity [12, 13, 14, 15]. It is also noticed that the strengthening process using SPD is a promising technique to enhance both mechanical and physical properties of pure metals or alloys [16, 17]. There are various available SPD processes nowadays; however, the ones which grabbed the most interest are the high-pressure torsion (HPT) and equal-channel angular pressing (ECAP) techniques [15, 18, 19, 20]. High-pressure torsion (HPT) is characterized by its ultimate fraction of high-angle grain boundaries (HAGBs) and very small grain size production [17, 21]. One way to achieve hardness homogeneity is through HPT discs via utilizing consecutive processing by adopting large number of revolutions [22, 23]. More comprehensive explanation and principles of the HPT can be found in [13, 21].

Based on a previous study [24], two most common SPD techniques, HPT and PM, are adopted to obtain a bulk of AA6061-15%SiC with ultra-hard nanostructured production. The effectiveness of HPT method in the production of ultimate refined grains within matrices of aluminum, particularly Al-based metal matrix composites (MMCs), was examined, evaluated and assessed. Particular type of composites was considered in this work, which is characterized by having ameliorated mechanical properties of modified consolidated ultrafine initial composite powders through refinement and retention. It is worth mentioning that the majority of past studies covering the processing of HPT for MMCs are with virtually qualitative conclusions. However, in the presented work, a quantitative evaluation approach was employed and adopted to discover the HPT processing conditions influence on the relative density, hardness, and microstructural observations of AA6061-15% SiC_p composite. Special consideration were devoted to the development of a generic method to explain the dependency interrelationship between the processing pressure of HPT and the implemented number of discs revolutions versus the composite mechanical properties. Mathematical models, to describe above-mentioned parameters interrelationships, were postulated and processed [25], using experimental data, to establish relevant three dimensional response surfaces and contours graphs. This is to reach a better trend understanding and to become as a prior digital database reference in the design stages.

Materials and Experimental Procedure

The matrix used in this work is based on micron-powders of AA6061 and reinforcement of SiC particulates having average sizes of 30 μm and 2 μm, respectively, where the as-received SiC powder had asymmetrical shape with a 1-to-5 μm range of sizes. The production of the AA6061-15%SiC_p composite was prepared by mixing specific percentages of both powders, AA6061 and SiC, in a vacuum ambient within a glove box. The next step was to employ a turbula blender in mixing at a 96 rpm rotational speed for three hours processing interval. Afterwards, a single sided uniaxial hot compaction (HC) process was applied for 30 minutes to the AA6061-15%SiC_p composite powders, through a cylindrical disc of diameter, height, temperature, and compaction pressure of 10 and 9.7 mm, 400 °C, and 525 MPa, respectively.

HPT was then adopted, as a secondary step for HC discs consolidation processing, where it was performed at room temperature utilizing the earlier explicated apparatus [26], Figure 1a. A lower die rotation was taking place to reach a fixed 1 rpm speed, in order to realize torsional straining. Marking was done for every disc upper surface separately right after HPT and before any hardness or microstructural analysis. HPT was performed at 1 or 3 GPa pressure utilizing constant 1 and 4 revolutions in a forward direction.

The mechanical properties, density, disc consolidation behavior before/after HPT were described. Average grain intercept (AGI) method was adopted to get the average grain and sub-grain size. Entire experimental procedures are diagrammatically explained by Figure 1b.

Sequential iterative nonlinear regression procedures were employed to get the most suitable mathematical relationships that express the relation-ship between the variables under study, as stated previously [24, 27]. Based on the set of experimental data obtained from hardness and compression tests in addition to the microstructure analysis which presented in Table 1, the appropriate models were postulated, developed, and finally examined against its adequacy and significance through ANOVA analysis [24]. Many statistical criteria such as correlation factor (factor of determination) R^2, $t_{statistics}$ value

FIGURE 1 Experimental set-up and procedures sequence

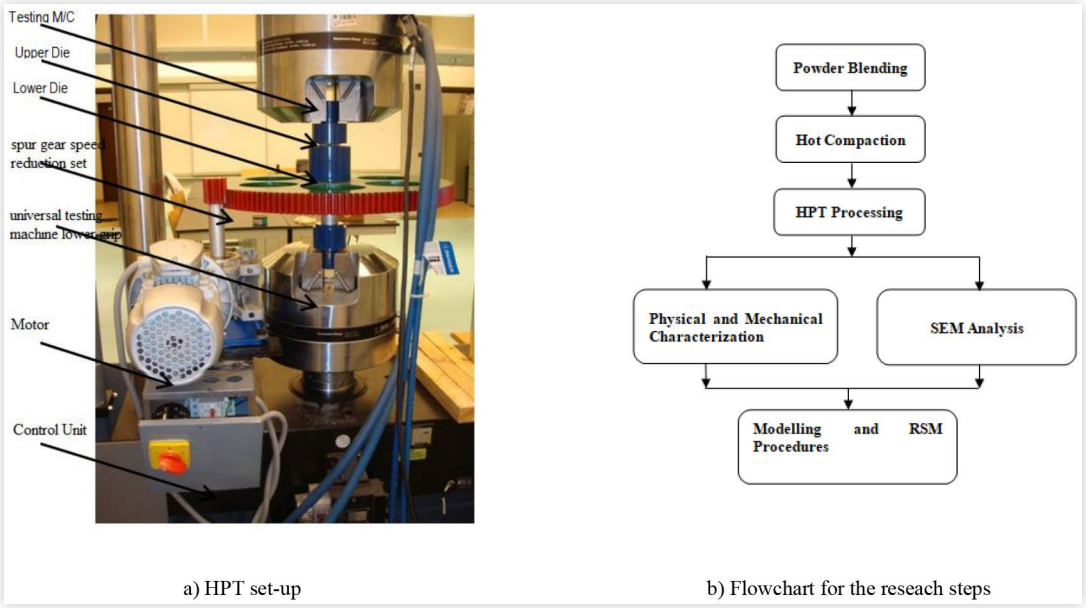

a) HPT set-up

b) Flowchart for the reseach steps

TABLE 1 Experimental data used in the analysis.

Condition		*N* = 0	*N* = 1	*N* = 2	*N* = 3	*N* = 4
P = 1 GPa	RD %	96.4	97.10	97.16	97.35	97.35
	Hv- at the center (R_0)	96.00	148.00	161.00	172.00	184.00
	Hv- at half the radius (0.5R)	96.00	172.50	194.00	198.00	202.00
	Hv- at the periphery (R)	96.00	201.00	205.00	206.00	209.00
	Yield stress σ_y (MPa)	305.00	370.00	386.00	398.00	409.00
	Compressive strength σ_c (MPa)	342.00	405.00	416.00	428.00	453.00
	Facture strain (ε_f%)	23.00	11.00	11.00	10.00	10.00
	Grain size μm	33.00	31.50	31.00	26.00	25.00
	Subgrain size μm	3.00	2.70	2.50	2.00	1.60
	Substracture size	420.00	260.00	243.00	225.00	184.00
P = 3 GPa	RD %	96.40	97.10	97.20		97.30
	Hv- at the center R_0	96.00	158.00	174.00		198.00
	Hv- at half the radius 0.5R	96.00	189.00	207.00		217.00
	Hv- at the periphery R	96.00	220.00	222.00		224.00
	Yield stress σ_y (MPa)	305.00	382.00	393.00		415.00
	Compressive strength σ_c (MPa)	342.00	412.00	424.00		461.00
	Facture strain (ε_f%)	23.00	10.00	10.00		9.00
	Grain size μm	33.00	24.50	24.00		24.00
	Subgrain size μm	3.00	2.20	1.90		1.60
	Substracture size nm	420.00	258.00	230.00		154.00

and F_{ratio} were used to judge the models' eligibility. To enhance understanding of the true functional dependence, and to give a quantitative assessment of the intended true interrelationships, the selected best models were implemented in terms of three-dimensional (3D) and contour graphs.

In the current analysis, the dependent variables were the relative density (RD), the mechanical properties; [Vicker's hardness (Hv), the yield strength (σ_y), the compressive strength (CS), and the fraction strain (ε_f)]; in addition to the microstructural evolution [the grains size (GS) and the subgrains size (SGS)]. The considered independent variables were the number of revolutions (N), distance from the processed disc center (R), and HPT processing pressure (P).

Results

Effect of the Processing Parameters on the Composite Relative Density

A relationship was created between the AA6061/SiC_p composites discs RD, and other two independent variables, represented in HPT processing N and P, using the fitting strategy mentioned previously, with the adoption of a set of experimental system described in Table 1. The statistical package for the social sciences (SPSS) was utilized to perform an iterative regression for this unconventional non-linear case following the criteria of default convergence. Numerical calculation and testing were taking place for the derivatives of the model versus the specified values of criteria. Iteration continued till reaching the finest model having the least residuals squares, related to the intended criteria. The results of this process led to the model:

$$RD\% = 96.52\left(N+1\right)^{(0.006)}, \qquad \text{Eq. (1)}$$

with R^2 of 88.5% along with parameters $t_{statistics}$ of 1149 and 6 together with F_{ratio} value of 2354166. Such excellent values confirmed the significance and adequacy of the developed model. While P was not significant enough to enter the relation, N yielded a slight effect of the RD.

Figure 2. examines the goodness of the resulting equation where predicted (estimated) values yielded from Equation 1 were compared to the experimental counterparts RD after processing through different processing parameters via HPT. It can observe from Figure 2a that predicted values are close to its counterparts the experimental ones, thus offering reliable estimation values regarding RD-N interrelationship. The residuals distribution for the HPT-processed discs RD is shown in Figure 2b where noting was observed against hypothesis that residuals are randomly distributed with zero mean. Comparison of the experimental and the predicted values at various processing revolutions are shown in Figure 3 which, also indicating an excellent predicted-experimental agreement, which confirm the model robustness.

Effect of the Processing Parameters on the Composite Hardness

A functional interrelationship (2) was established between the dependent variable, the alloy of Hv-values, and the influential independent variables, R, N, and P. While (R_0) represents the position at the disc centre, ($R_{0.5}$) and (R_1) determine the locations at midway between the disc centre, and that at the periphery respectively. The best model was in the form:

$$Hv = 108.58\left(N+1\right)^{(0.369)}\left(R+1\right)^{(0.277)}, \qquad \text{Eq. (2)}$$

with good statistical criteria of R^2 of 77% along with parameters $t_{statistics}$ values of 14, 7.4 and, 3 together with F_{ratio} value of 529. Figure 4a is dedicated to indicating how predicted (estimated) values are close to vits counterpart experimental values. In addition, the residuals distribution for the Hv-values is shown in Figure 4b. Model (2) implies that the HPT processing pressure was not effective enough to impose its possible effect on Hv-values. Comparisons between the Experimental and predicted effects of the number of revolutions and the position

FIGURE 2 Experimental results vs. predicted of the RD for the HPT-processed discs as depicted at (a) and Residuals distribution at (b).

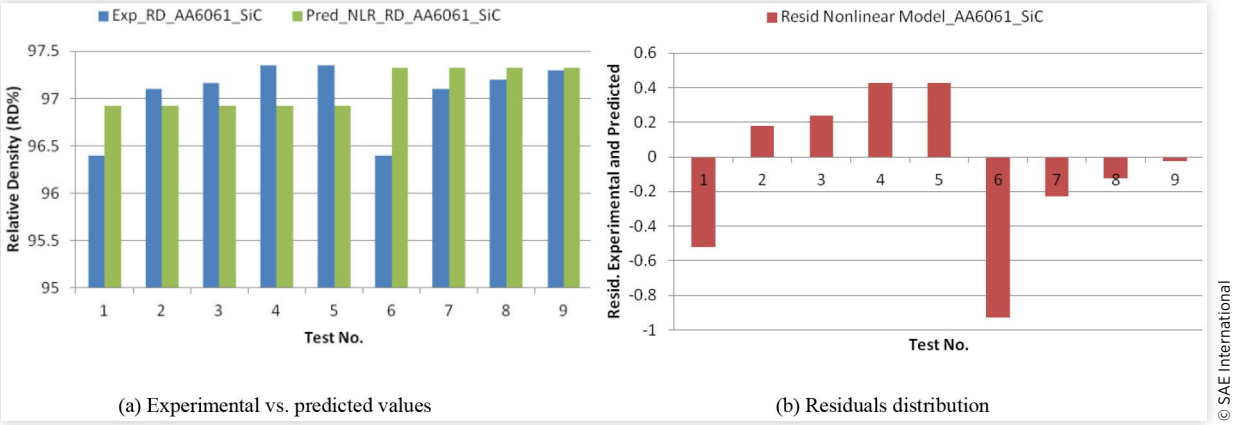

(a) Experimental vs. predicted values (b) Residuals distribution

FIGURE 3 The effect of HPT processing pressure and number of revolutions on RD of AA6061/SiC_p disc compared to the predicted RD-values from model (1).

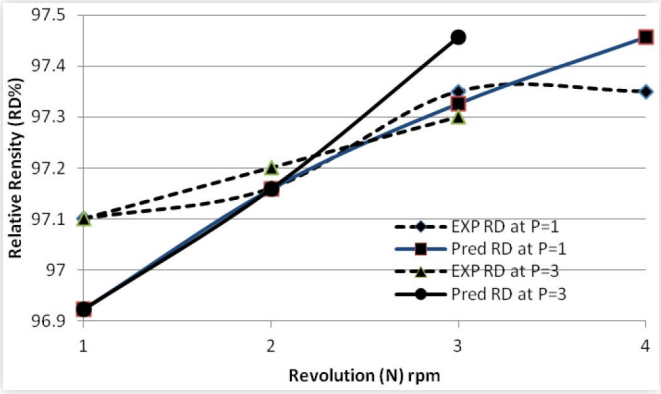

from the centre of disc on Hv-values at different processing pressures for AA6061-SiC_p are presented in Figure 5.

It is noticed that the predicted (estimated) values are close to its counterpart experimental values for the AA6061 composite discs processed at a pressure of 1 and 3 GPa. It is clear that when hardness values are higher at the peripheral regions, they are lower at the centers of discs. Also, it could be deducted from the reached results that augmenting the Hv-values along with applied pressure was a consequence of elevated Hv-values formation all-around the discs peripheries, subsequently, a homogeneous distribution of high hardness zone swept across the discs. Similar agreement with was reached [28] regarding the effect of Hv-values of discs processed by HPT through cross section area of AA6061-SiCp attitude concerning material states of low stacking faults energy (SFE) and face-cantered cubic (FCC) structure. Hardness values were found to be lower at the discs centre and higher at peripheries. In addition, Figure 5 shows that the Hv-values of the AA6061-SiCp composite discs processed at 1 GPa at a different number of revolutions were very close to the counterparts processed at 3 GPa. The insignificant increase in the Hv-values noticed in the discs processed at 3 GPa compared to that within the 3 GPa applied pressure.

Figure 6 indicates response surfaces and contours for each of the experimental results and the corresponding expected values using model (2). The functional Hv-N-R relationships are well qualitatively explained. It is shown a strong influence of both N and R on the deformed product. However, surfaces indicate that Hv nonlinearly increases as each of N and R increases with a higher slope for N.

A quantitative evaluation of the results is diagrammatically expressed in details within Figure 5. It is shown that using 1-revolution lead to augmenting the AA6061/SiC_p composite Hv-values to 210 at the disc peripheries from 150 at the centre. This finding could be a great indication for that lacks of properties distribution homogeneity all-around the disc cross-section. On the other hand, this lack of homogeneity in hardness vanished bit by bit by additional straining up to 4-revolutions, resulting in an average constant Hv value over the entire disc of 217, which could be stated as reasonable. This outcome means that the Hv-values increased by ~126% post HPT processing compared to the un-processed counterparts (Hv = 96) as shown in Figure 5. It should be noted that, for AA6061/SiC_p composite compared to AA6061discs [29], 4-revolutions were not enough to achieve full homogeneity in the composite discs and the maximum Hv-values did not change significantly with increasing the strain.

For the sake of reaching a better explanation for the rotation effect on hardness, a relationship between hardness variations ($Hv_{variation} = Hv_{\_N=0} - Hv_{\_N=1,2,3,4}$) and both the influential parameters N and R was established to have the form:

$$Hv_{variation} = 68.77N^{0.146}(R+1)^{0.612}, \qquad \text{Eq. (3)}$$

with R^2 = 77.1%; $t_{statistics}$ = 16, 3.17, 6.58; and F_{ratio} = 558, the developed model (3) is found reasonable enough to represent the experimental data.

Figure 7 indicates the hardness variation attitudes as it has been affected by N and R using both the experimental data, Figure 6a, and those extracted from model (3), Figure 7b. As can be seen from response surface topography and contour maps, an accurate quantitative and qualitative correlation is obtained. Vickers's hardness is prominently influenced by each of N and R especially at N ≥ 3 and R ≥ 0.5.

FIGURE 4 Experimental results vs. predicted data of the Hv-values for the HPT processed discs as depicted at (a) and Residuals distribution at (b).

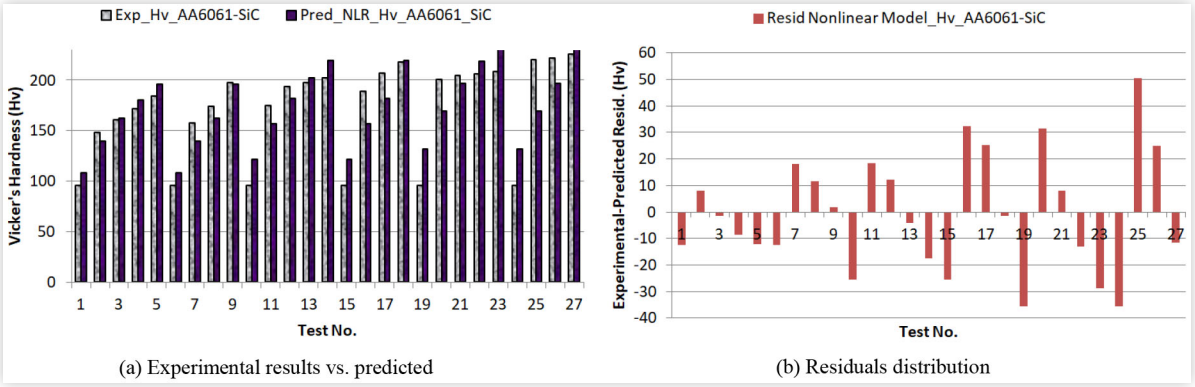

(a) Experimental results vs. predicted (b) Residuals distribution

FIGURE 5 Effect of number of revolutions (N) on Hv-values of AA6061-SiCp composite disc processed at (a) 1 GPa, (b) 3 GPa compared to (c) the obtained from model (2).

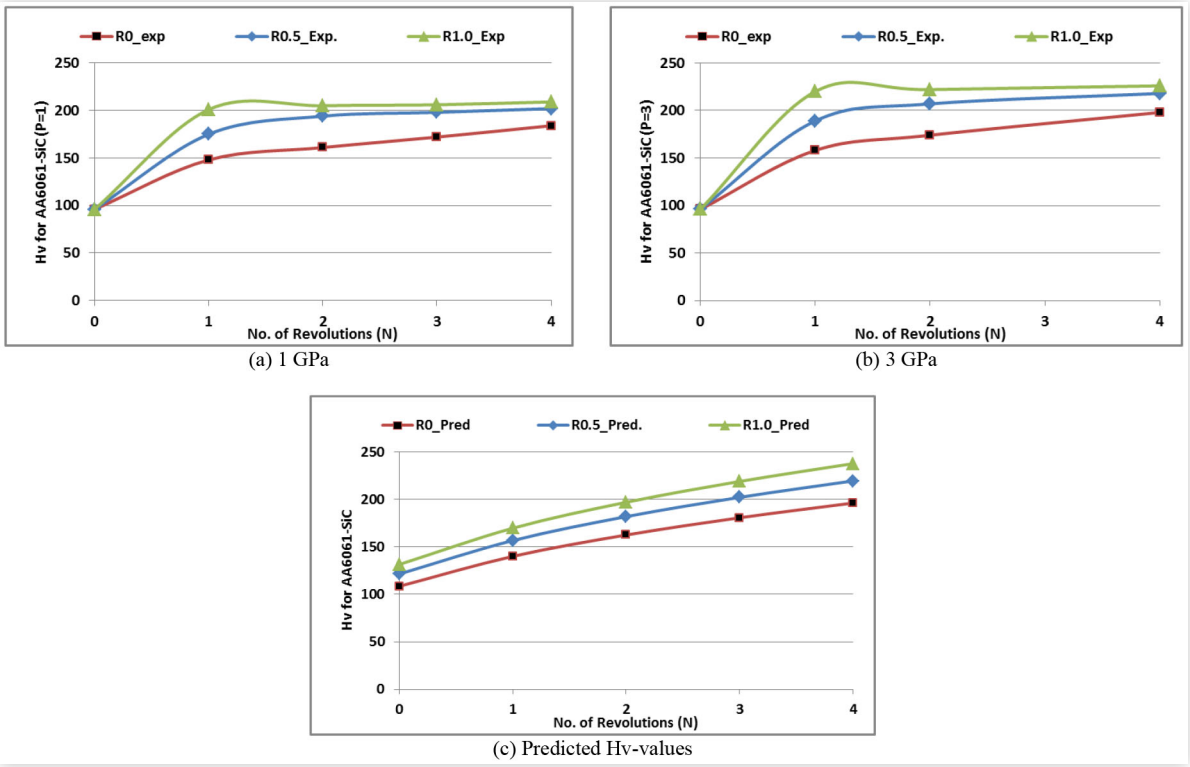

FIGURE 6 Response surface and contours for Hv of AA6061/SiCp discs processed via HPT.

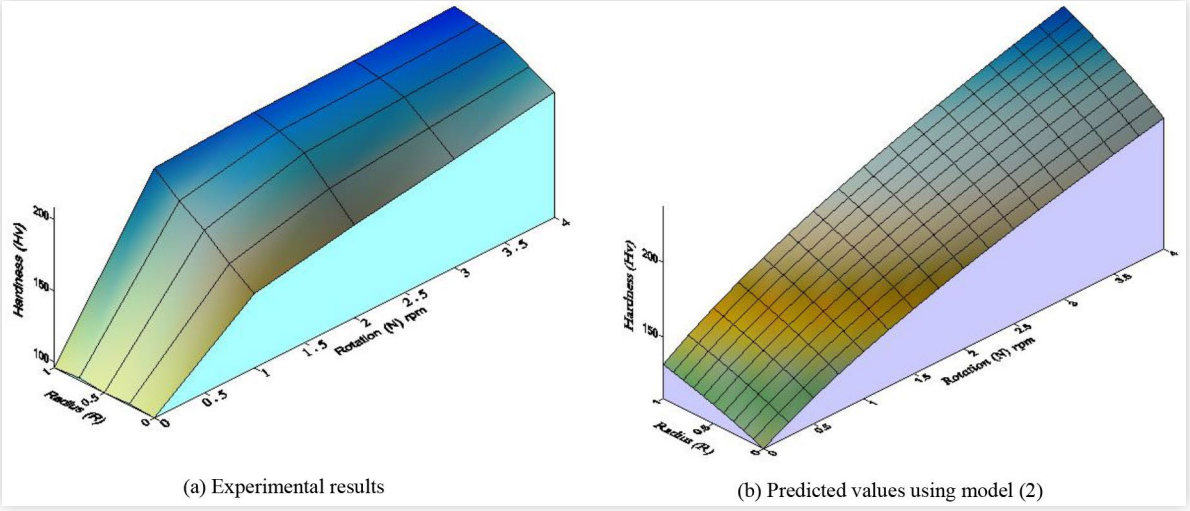

Effect of the Processing Parameters on the Composite Compressive Properties

Similar fitting procedures and strategy were employed to develop a functional interrelationship between σ_y; model (4), the CS; model (5), and ε_f; model (6) as dependent variables and both of N, and P as influential independent variables for AA6061-SiC_p composite.

$$\sigma_y = 317.93(N+1)^{(0.172)} \quad \text{Eq. (4)}$$

with R^2 of 90.6% along with $t_{statistics}$ of 39.5 and, 7.8 together with F_{ratio} value of 3467.

$$CS = 350.62(N+1)^{(0.165)} \quad \text{Eq. (5)}$$

FIGURE 7 Hardness variations of the (a) experimental results vs. the (b) predicted values, as affected by R and N.

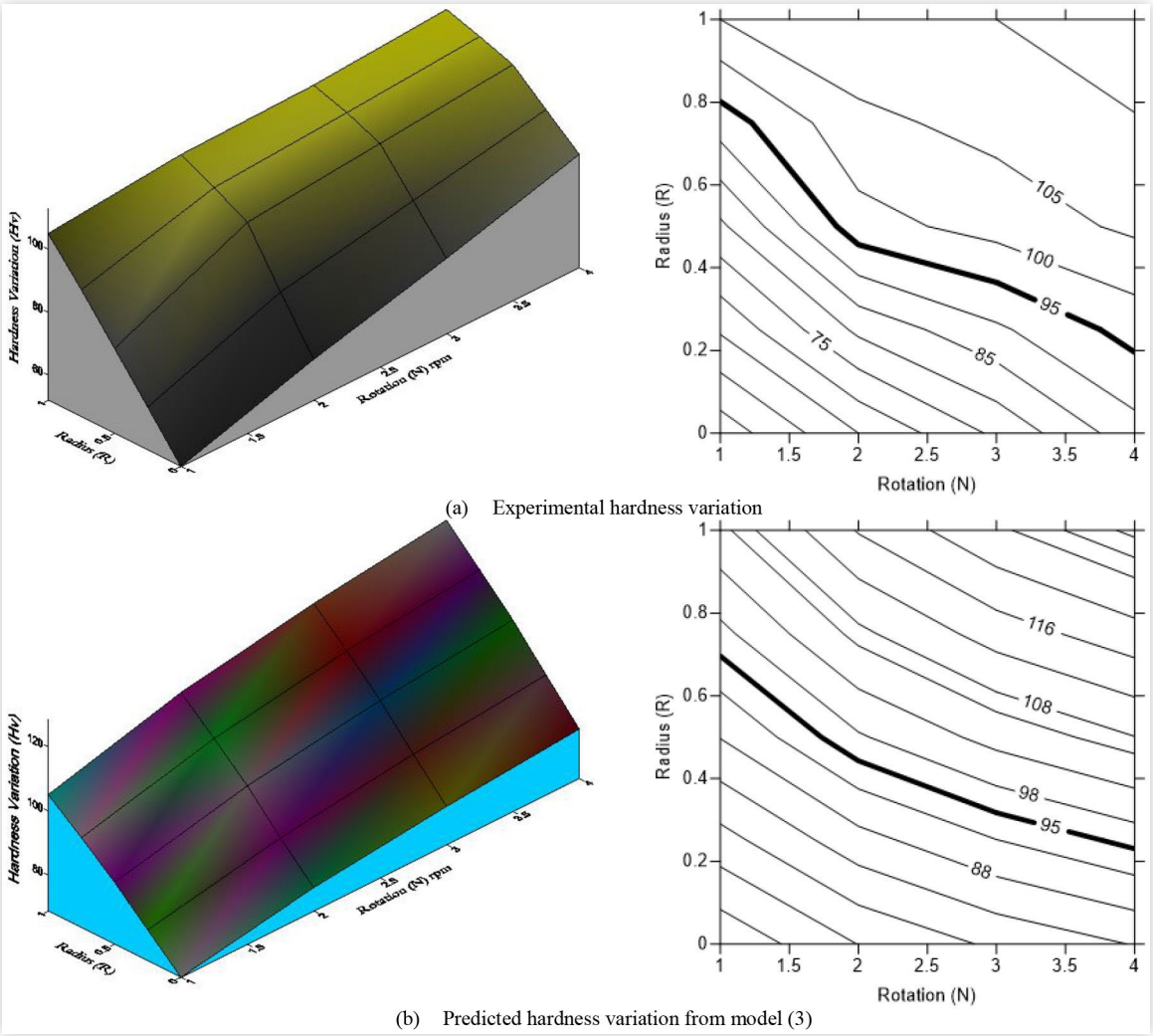

with R^2 of 94% along with $t_{statistics}$ of 52.6 and, 10.3 together with F_{ratio} value of 6082.

$$FS = 21.85(N+1)^{(-0.664)} \quad \text{Eq. (6)}$$

with R^2 of 86.4% along with $t_{statistics}$ of 14.3 and, −6.8 together with F_{ratio} value of 174.

Accordingly, it is clear that the developed models (4-to-6) are regarded as significant and satisfactory for the relevant functional interrelationship representation. Once more, the imposed pressure was not significant enough to enter the equation as an influential parameter on any of the yield strength, the compressive strength or the fracture strain.

Figure 8a, c, and e show the similarity between the predicted (estimated) values and experimental values for the yield strength, compressive strength, and fracture strain. In addition, the residuals distribution of the compressive properties is shown in Figure 8b, d, and f.

For practical predictability, Figure 9 represents how the values of the predicted (estimated) model are close to the experimental ones for both the yield stress (Figure 9a), the compressive strength (Figure 9b), and the fracture strain (Figure 9c). From the models (4-to-6) it is clear that the HPT processing pressure had insignificant influence on the compressive properties. It can be said that, the properties of deformed AA6061-SiC_p discs of compressive and yield strengths were considerably greater than the un-deformed. Meanwhile, compressive and yield strengths of HPT-processed discs augmented considerably with augmenting the imposed strain, which was accompanied with a decrease in the ductility.

Effect of the Processing Parameters on the Composite Grains, Subgrains Substructure Size

Scanning electron microscopy (SEM) analysis was employed in order to investigate the internal structure of AA6061/SiC_p composite HCs discs before and after HPT processing. The as-HC discs microstructure of AA6061 composite is displayed

FIGURE 8 Experimental results vs. predicted data and the residuals distribution of the yield strength, compressive strength, and fracture strain for the AA6061/SiC_p processed discs.

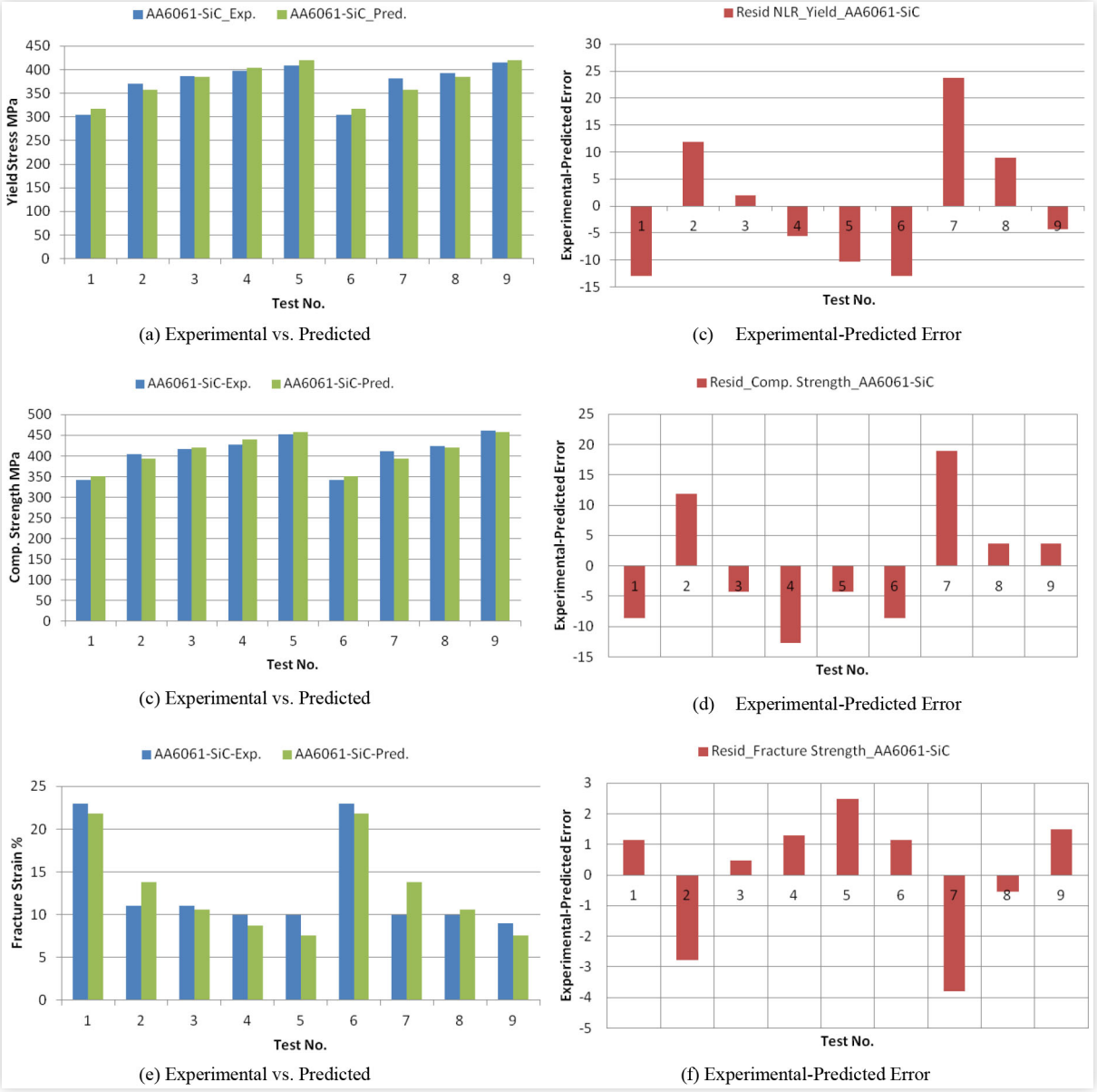

(a) Experimental vs. Predicted

(c) Experimental-Predicted Error

(c) Experimental vs. Predicted

(d) Experimental-Predicted Error

(e) Experimental vs. Predicted

(f) Experimental-Predicted Error

in Figure 10. Figure 11 shows the development in the microstructure at the peripheries of the surface of discs after HPT processing through 1-rev. (a, c), and 4-rev. (b, d) at a pressure of 1 GPa (a, b) and 3 GPa (c, d), respectively.

SEM micrographs confirmed a potential of achieving UFG after HPT processing. Influence of the amount of strain, formed during deformation, on the size and shape of the substructure, subgrains, and grains was clearly depicted at the displayed micrographs, which was achieved via augmenting the revolutions from 1-up to-4. The average grains, subgrains, and substracture sizes of the HC was 33, 3 μm, and 420 nm, respectively. HPT straining via $\varepsilon_{eq} = 1.57$ (corresponding to N = 1-rev.) resulted in refining the sizes of substructure to 260 nm, subgrains to 2.7 μm, and grains to 31.5. Moreover, Increasing the amount of strain up to $\varepsilon_{eq} = 3.1$ (4-rev.) exposed additional refinements of substructure to 184 nm, subgrains to 1.9 μm, and grains to 25 μm. (Figure 10a, b).

When the processing pressure of HPT was augmented from 1 till a maximum of 3 GPa, an extra minor substructure, subgrains, and grains refinement was achieved. This could be attributed to the SPD induced with augmenting number of revolutions till a maximum of 3 GPa, where an elongation in various ways was taking place in the consolidated powders equiaxed subgrains following the slip planes orientation, as shown in Figure 7d. HPT processing via 4-revolutions at 3 GPa showed additional refinement of the of the substructure to 154 nm, subgrains to 1.5 μm, and

FIGURE 9 Experimental results vs. predicted ones of the yield stress, compressive strength, and fracture strain of AA6061/SiCp processed via HPT.

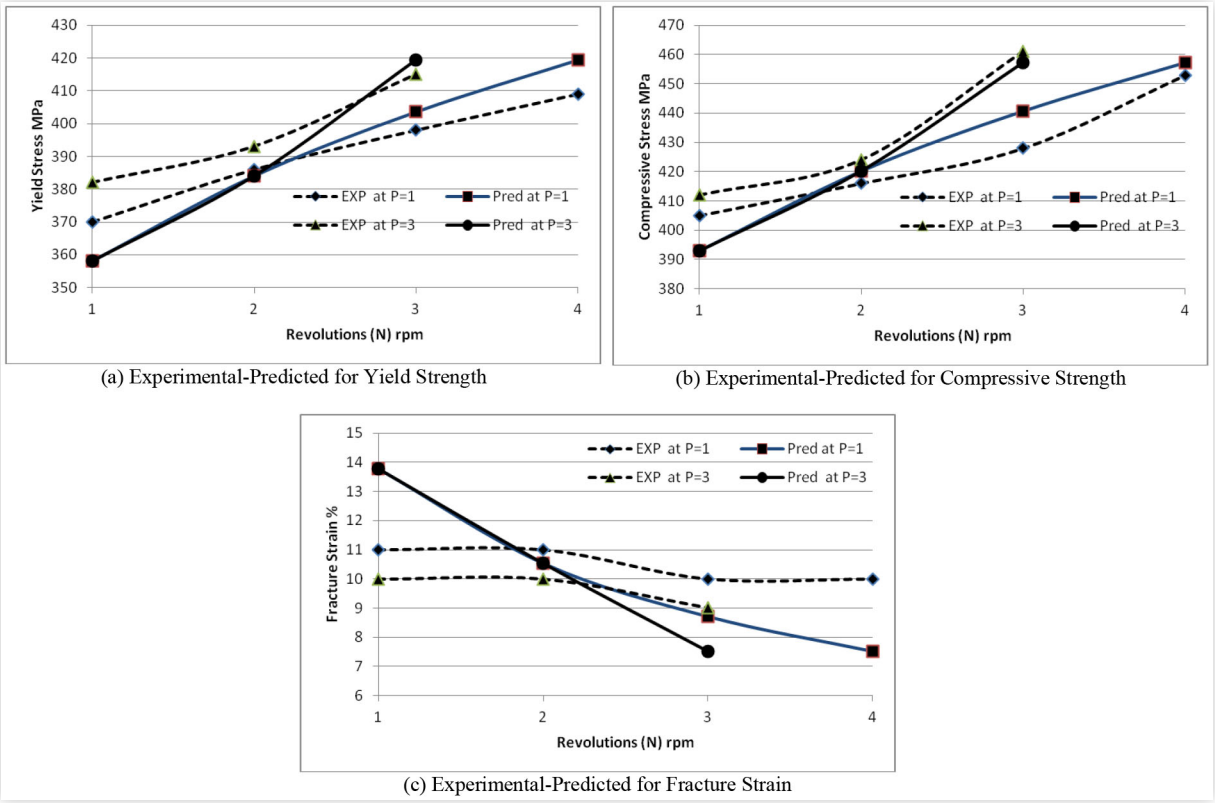

(a) Experimental-Predicted for Yield Strength

(b) Experimental-Predicted for Compressive Strength

(c) Experimental-Predicted for Fracture Strain

FIGURE 10 SEM micrographs of the HCs discs for AA6061/SiCp composite, with arrows pointing at the triple junctions of SiCp and alongside GBs.

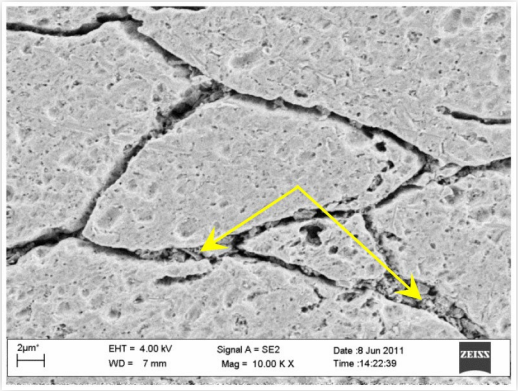

grains to 24 µm. The arrangement of the particles of SiC alongside the boundaries of grains of the consolidated sheared grains augmented the deformation resistance around the ceramic hard particles; therefore, the strain hardening increased, which could be interpreted by having a dynamic recovery act. Both dynamic recovery and strain hardening could be the reason behind the noticeable augmented refinement when the imposed pressure augmented from 1 GPa (Figure 10a, b)-to-3 GPa (Figure 11c, d), which is related the high subgrain level disorientation.

As shown in Figure 11, the deformation amount was clear through the alignment in the shear orientation of the AA6061/SiC_p consolidated grains, which augmented with augmenting the number of revolutions and/or the imposed pressure. The equiaxed subgrains of the consolidated powders were noticed to have been prolonged in various ways following the slip planes, due to the induced SPD when strain is greater; as shown in Figure 11d. Moreover, regarding the same grain, different subgrains coordination exhibited deformations in multiple slip zones, which is a clear indicator of the case of multiple slips. The different orientation of the grains made it more difficult for the dislocation to change its direction of motion which resulted in increasing the hardness and the strength of the processed disc. As a result, this could be considered as an indicator for a probable evolution in the substructure from medium-to-high angle boundaries. More research and examinations via transmission electron microscopy (TEM) are essential for this claim validity.

The fitting procedures have led to the following nonlinear functional interrelationship between the alloy grain, subgrain, and substructure size (GS, SGS, and SSS, respectively), as a dependent variable, and N and P, as influential independent variables.

$$GS = 33.52(N+1)^{(-0.197)} \quad \text{Eq. (7)}$$

FIGURE 11 AA6061/SiC composite discs SEM micrographs, processed at 1 GPa (a, b) and 3 GPa (c, d) via (a, c) 1-revolution, and (b, d) 4-revolutions, respectively.

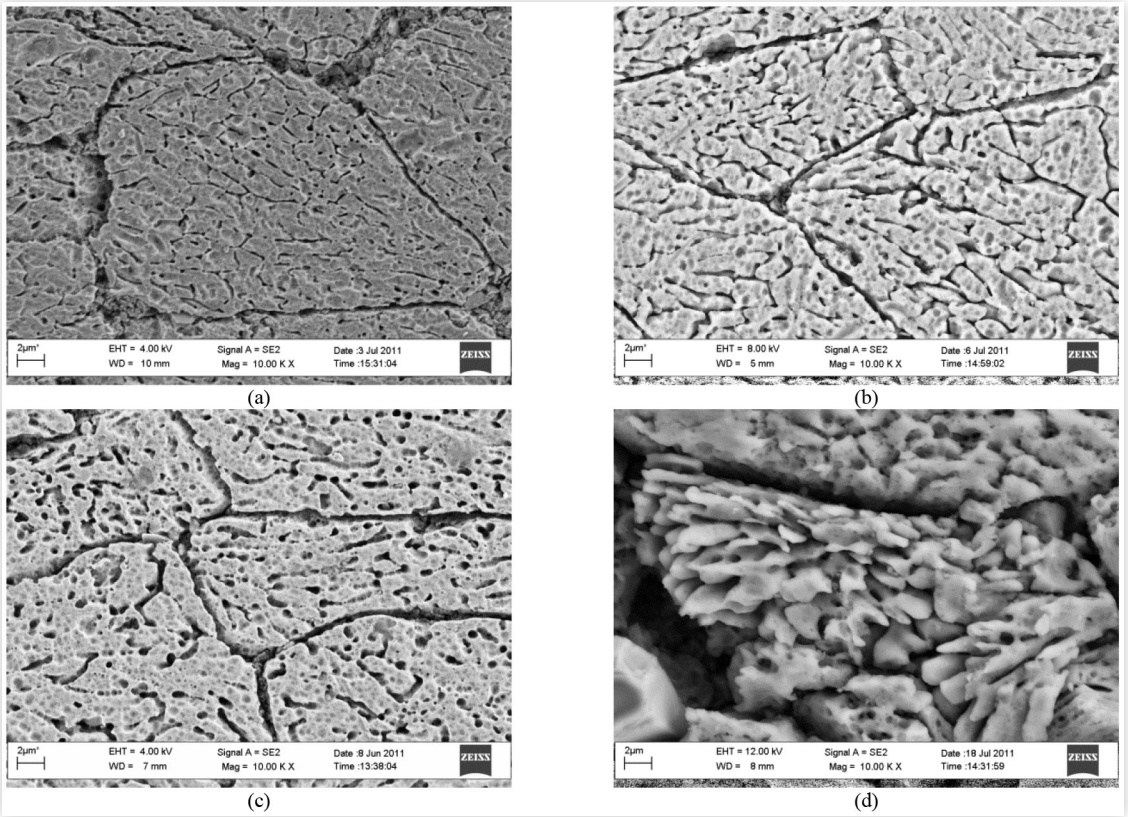

with R^2 of 64% along with $t_{statistics}$ = 125 and, –3.6 together with F_{ratio} value of 471, the obtained model is an appropriate relevant representation of the functional interrelationship.

$$SGS = 3.04(N+1)^{(-0.341)} \quad \text{Eq. (8)}$$

with R^2 of 84% along with $t_{statistics}$ = 19.5 and, –6 together with F_{ratio} value of 427, the model is adequate and satisfactory.

$$SSS = 412.655(N+1)^{(-0.539)} \quad \text{Eq. (9)}$$

with R^2 of 96% along with $t_{statistics}$ = 30 and, –12.5 together with F_{ratio} value of 838, therefore, it is concluded that it is appropriate, well significant, and satisfactory to be used for the representation of experimental data.

Figure 12 shows the experimental and the counterpart predicted results comparison. Also, residual values and distribution for each parameter are included. The influence of the HPT processing pressure and a number of revolutions on microstructural evolutions for AA6061 compared to the predicted values from models (7-to-9) is shown in Figure 13.

Discussion

Based on the RD findings (Figure 3), some obvious and important trends for materials processed by HPT have been emerged. All AA6061/SiC_p composite discs processed via HPT revealed higher RD compared to the hot compacted counterparts (The RD produced for the as-HC condition was 96.4). Increasing the number of revolution imposed greater strain leading to an increase in RD of the AA6061/SiC_p due to the huge shear deformation applied. Greater shear deformation usually facilitates the reduction porosity as: particles deformation, in addition to its travel into voids, and flatting of the submicroscopic and microscopic characteristics on the surface of particle [29]. This can be correlated to the main part of shear strain action on consolidation process based on particles realignment, mechanical interlocking, and localized fragmentation. In addition, the shear deformation may result in breaking-down the oxide layers, naturally created on the Al-powder particles surface, which cause a main delay for the effective bonding during sintering of Al-powder particles [30]. Breaking off this barrier can enhance diffusion [30]. Besides, the huge local diffusion reduction among Al-particles without reinforcement was obvious, as a result of the build-up on the aluminium matrices particles of fine SiC particles. The presence of various SiC particle sizes, if linked to the particles of Al matrix, leads the absence of uniformity in the reinforcement distribution within the matrix; therefore, an obvious density drop occurred.

Various mechanisms are adopted for strengthening when using SPD, which could involve strain hardening, solid

FIGURE 12 Experimental results vs. predicted and the residuals distribution for grains size, sub-grains size, and substructure size.

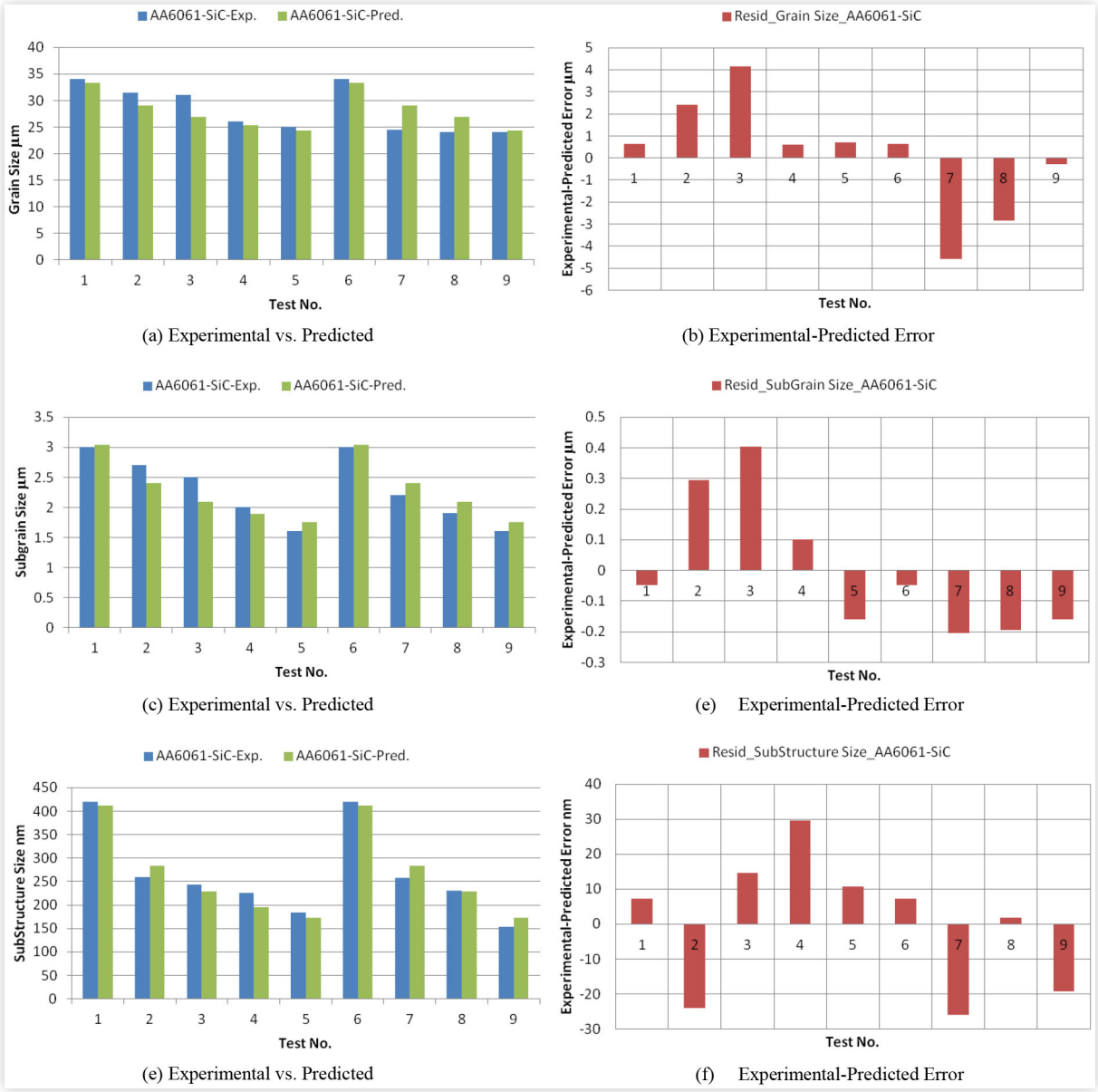

solution, oxide dispersion, and grain refinement [31, 32, 33]. Strengthening the alloy could be explained by the substitution and interstitial solute atoms of the elements in alloying of AA6061, which in its turn alter the crystal lattice and delay dislocation mobility. The great level of strain produced through HPT usually leads to the creation of ultimate dislocations density, which interacts effectively with the pinning solute and secondary phases in AA6061 consolidated particles at their boundaries by SiC particles [34]. It should be stated that with the addition of SiC there has been a reduction in grain size of the processed AA6061, where the particles of SiC supported in the refinement of grains by restraining their boundaries relocation [35]. In addition, SiC particles usually help to delay the grain growth. Moreover, higher strength and hardness were obtained as a result of cumulative dislocation at the boundaries, which in its turn lead to augmented resistance to deformation. As a result of the high proportion of deformation per revolution, it could be deduced that the huge amounts of dislocations were created so that the common dislocations interaction reach an improvement and the boundaries of subgrain grow into grain boundaries with large angles of disorientation, which is usually assisted with dynamic recovery [33].

Dislocation strengthening assisted significantly in the strength and hardness enhancement of the HPT processed discs. The additional dislocations through subgrain and grains boundaries make the dislocation slip harder. The density of dislocation typically augments with HPT processing, as a result

FIGURE 13 The effect of HPT processing pressure and number of revolutions on grains, subgrains, and substructure size of AA6061/SiCp composite compared to the predicted values from models (7-to-9).

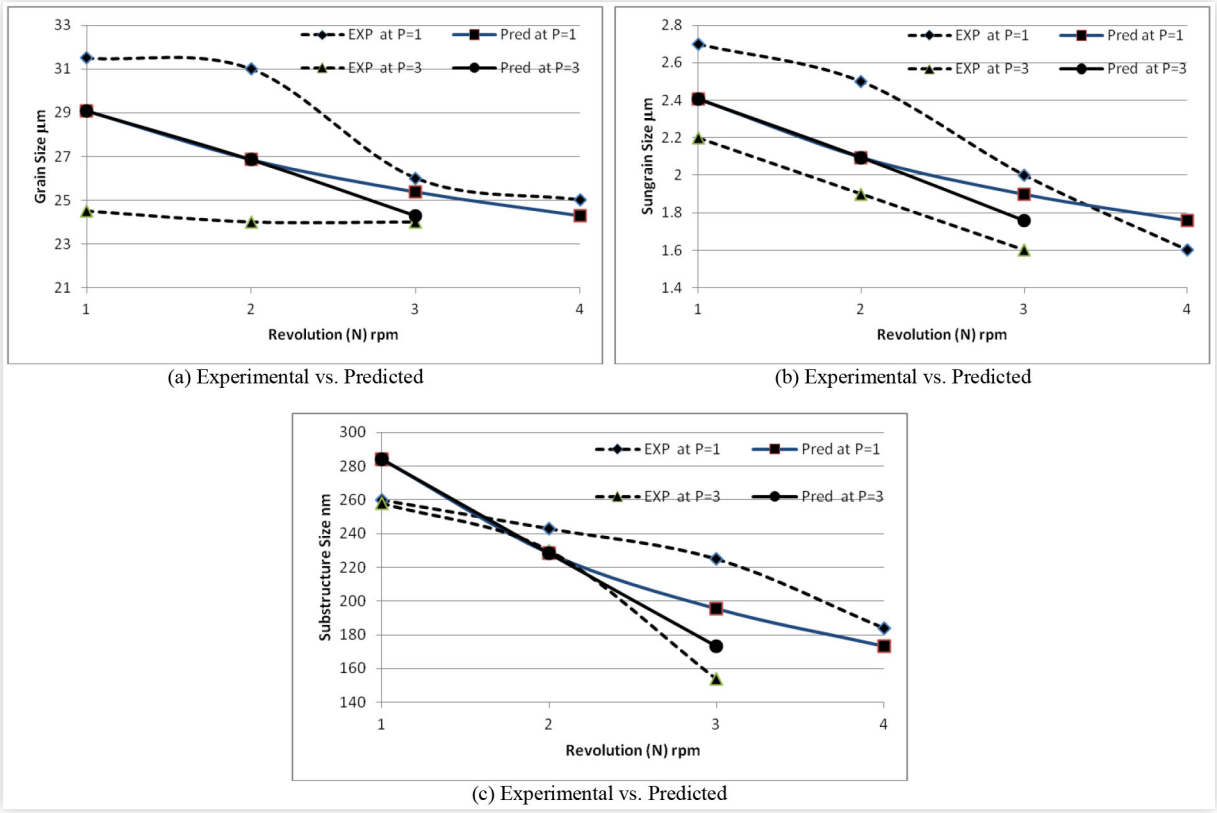

(a) Experimental vs. Predicted

(b) Experimental vs. Predicted

(c) Experimental vs. Predicted

of the occurrence of multiplication or new dislocations; therefore, the dislocation motion is impeded by other dislocations, which is correlated with the hardness substantial increase after HPT processing [32, 36, 37]. The SiC reinforcement led to additional stuck dislocations in the grain boundaries and interior [33, 38]. Therefore, the imposed stress required for metal deformation increased with increasing cold work, and hence the composite showed higher strength and hardness than the alloy.

It is worth mentioning here that even though the adoption of the reinforcement of SiC ameliorated the overall hardness of discs, relative to the monolithic alloy; it helped in increasing the hardness distribution inhomogeneity even after 4-revolution. This finding could be correlated to the augmented hard-SiC particles friction at the interfaces of discs-die wall, which resulted in a strain hardening amelioration at the discs peripheries compared to centers. When composite discs were subjected to SPD, it could be also deduced that the SiC particles fragmentation, on the relatively soft Al-matrices, all along the boundaries and their impingement was a sign of the resulted ultimate strain hardening.

It could be said that after HPT processing, according to the Hall-Petch law, the noticeable enhancement in the strength of material is mostly related to the homogeneous ultra-fine grained (UFG) microstructure formation, which could lead to a major strengthening [39]. In addition, finer grains size usually increases the grain boundaries area that impedes dislocation motion. As a result, the formation of these pile-ups would lead to a concentration of stress onward their slip planes; consequently, adjacent grains would have new dislocations [38]. It is worth mention here that dislocations take place more often at grain boundaries (GBs) and interiors with the repeated revolutions of HPT, which could be attributed to the large strain and solute effect. When the density of dislocation topped to a critical value with the augmenting in strain, the disorientation through the subgrains augmented as a result of accumulation and annihilation of dislocation. On the other hand, the disorientation ultimately was developed quite sufficient to change from low-angle grain boundaries (LAGBs) to high-angle grain boundaries (HAGBs) [40], which would lead to increasing the compressive properties.

In addition, it should notice that there are several important phenomena resulting from the difference in mechanical and physical properties of the metal matrix and ceramic reinforcement phase. The main difference in the thermal expansion coefficients (CTE) between the reinforcement and matrix arouse when using the required high temperatures of HC process, which produces residual stresses within the material after cooling. Dislocations are suggested to be created within the matrix when increasing pressure. This could be attributed to compressibility differences between reinforcement and matrix. Moreover, this obtained pressure, resulted from inside matrix dislocations, is considered the same as the one produced from dislocation during thermomechanical processing, resulting from CTE mismatch among the two phases [41].

Conclusion

A fabrication of AA6061 discs with a reinforcement of 15% SiC_p was successfully achieved, through a hot compacted mixed powders assortment going through a process of high pressure torsion to nearly 97.3% of the theoretical density. The process of high pressure torsion was accomplished at different settings, where multiple numbers of revolutions were adopted, along with various levels of pressures. Structures of non-linear models were presented using a strategy for the sequence of favorite selection and reliable statistical measures, to examine the prediction capacity and dependency of the model, while examining and analyzing the residuals trends. The next deductions could be concluded out of the performed effort of this article:

1. Processing under one revolution led to a case of strain hardening being distributed in an inhomogeneous pattern, which found to be most effective and higher at the peripheries of the disc. On the other hand, it was reduced slowly when going to the center.
2. The uniformity in the distribution of hardness throughout the discs increased with increasing the equivalent strain.
3. The Vicker's hardness values of the hot compacted discs increased by 126% after the process of high pressure torsion for the consolidated powders of $AA6061/SiC_p$.
4. The processing of high pressure torsion produced a structure, which is described as a trimodel having microscale and subgrains, and nanoscale substructure. High pressure torsion processing at 3 GPa through 4 revolutions revealed significant grain refinement of average grain, subgrain and substructure sizes of 24, 1.5 μm, and 154 nm, respectively.
5. Structures of non-linear models were presented using a strategy for the sequence of favorite selection and reliable statistical measures, to examine the prediction capacity and dependency of the model.
6. Regarding the investigated experimental data, all the developed models were found to be significant and adequate to act as a good prediction tool for the data domain under investigation. A universal model can be then reached, whenever the experimental domain is widened.
7. The developed models indicated that the imposed pressure was not significant enough, to enter the equation as an influential parameter.

Acknowledgement

The authors would like to thank and acknowledge the continuous financial provision and help of Youssef Jamil Science and Technology Research Center (YJSTRC) and the Mechanical Engineering Department at The American University in Cairo-Egypt. The authors want also to appreciate the great effort of their lab engineers, who were very keen to provide all the necessary means to accomplish this work, and the research assistances, who gave their time and effort to reach the best out this work.

Nomenclature

HPT - high-pressure torsion

AA6061 - aluminum alloy 6061

SiCp - silicon carbide particles

Hv-values - Vicker's hardness values

AMCs - aluminum matrix composites

Al - aluminum

PM - powder metallurgy

SPD - severe plastic deformation

ECAP - equal-channel angular pressing

MMCs - metal matrix composites

HC - Hot compaction

AGI - average grain intercept

ANOVA - analysis of variance

R^2 - R-squared

$t_{statistics}$ - the ratio of the departure of the estimated value of a parameter from its hypothesized value to its standard error

F_{ratio} - test statistic for multiple independent variables

RD - relative density

σ_y - yield strength

CS - compressive strength

ε_f - fraction strain

GS - grains size

SGS - subgrains size

N - number of revolutions

R - distance from the processed disc center

P - high pressure torsion processing pressure

SPSS - statistical package for the social sciences

R_0 - represents the position at the disc centre

$R_{0.5}$ - represents the position at the disc half centre

R_1 - represents the position at the disc periphery

$Hv_{variation}$ - difference in vicker's hardness value

$Hv_{\_N\ =\ 0}$ - vicker's hardness value measured before disc processing

$Hv_{\_N\ =\ 1,2,3,4}$ - vicker's hardness value measured after disc processing via 1-up to-4 revolutions

SFE - stacking faults energy

FCC - Face centered cubic

UFG - ultra-fine grained

GBs - grain boundaries

LAGBs - low angle grain boundaries

HAGBs - high angle grain boundaries

CTE - thermal expansion coefficients
SEM - scanning electron microscopy
SSS - substructure size
TEM - transmission electron microscopy

References

1. Kunčická, L., Lowe, T.C., Davis, C.F., Kocich, R. et al., "Synthesis of an Al/Al_2O_3 Composite by Severe Plastic Deformation," *Materials Science & Engineering A* 646:234-241, 2015, http://doi.org/10.1016/j.msea.2015.08.075.
2. Carvalho, O., Buciumeanu, M., Madeira, S., Soares, D. et al., "Optimization of AlSi-CNTs Functionally Graded Material Composites for Engine Piston Rings," *Mater. Des.* 80:163-173, 2015, http://doi.org/10.1016/j.matdes.2015.05.018.
3. Alhashmy, H.A. and Nganbe, M., "Laminate Squeeze Casting of Carbon Fiber Reinforced Aluminum Matrix Composites," *Mater. Des.* 67:154-158, 2015, http://doi.org/10.1016/j.matdes.2014.11.034.
4. Jahedi, M., Paydar, M.H., and Knezevic, M., "Enhanced Microstructural Homogeneity in Metal-Matrix Composites Developed under High-Pressure-Double-Torsion," *Materials Characterization* 104:92-100, 2015, http://doi.org/10.1016/j.matchar.2015.04.012.
5. Ci, L.J., Ryu, Z.Y., Jin-Phillipp, N.Y., and Rühle, M., "Investigation of the Interfacial Reaction between Multi-Walled Carbon Nanotubes and Aluminum," *Acta Mater* 54(20):5367-5375, 2006, http://doi.org/10.1016/j.actamat.2006.06.031.
6. Bakshi, S.R., Lahiri, D., and Agarwal, A., "Carbon Nanotube Reinforced Metal Matrix Composites - A Review," *International Materials Reviews* 55(1):41-64, 2010, http://dx.doi.org/10.1179/095066009X12572530170543.
7. Kurita, H., Kwon, H., Estili, M., and Kawasaki, A., "Multi-Walled Carbon Nanotube-Aluminum Matrix Composites Prepared by Combination of Hetero-Agglomeration Method, Spark Plasma Sintering and Hot Extrusion," *Mater. Trans.* 52:1960-1965, 2011, http://doi.org/10.2320/matertrans.M2011146.
8. Bozic, D., Dimcic, B., Dimcic, O., Stasic, J. et al., "Influence of SiC Particles Distribution on Mechanical Properties and Fracture of DRA Alloys," *Mater. Des.* 31(1):134-141, http://doi.org/10.1016/j.matdes.2009.06.047.
9. Tan, M.J. and Zhang, X., "Powder Metal Matrix Composites: Selection and Processing," *Mater. Sci. Eng. A* 244(1):80-85, 1998, http://doi.org/10.1016/S0921-5093(97)00829-0.
10. Viswanathan, V., Laha, T., Balani, K., Agarwal, A. et al., "Challenges and Advances in Nanocomposite Processing Techniques," *Materials Science and Engineering R* 54(5-6):121-285, 2006, http://doi.org/10.1016/j.mser.2006.11.002.
11. Valiev, R.Z., Islamgaliev, R.K., and Alexandrov, I.V., "Bulk Nanostructured Materials from Severe Plastic Deformation," *Prog. Mater.* 45:89-103, 2000, http://li.mit.edu/S/td/Paper/Valiev00.pdf.
12. Dimić, I., Cvijović-Alagić, A., Völker, B., Hohenwarter, A. et al., "Microstructure and Metallic Ion Release of Pure Titanium and Ti-13Nb-13Zr Alloy Processed by High Pressure Torsion," *Mater. Des.* 91:340-347, 2016, http://doi.org/10.1016/j.matdes.2015.11.088.
13. Edalati, K. and Horita, Z., "A Review on High-Pressure Torsion from 1935 to 1988," *Materials Science & Engineering A* 652:325-352, 2016, http://doi.org/10.1016/j.msea.2015.11.074.
14. Cepeda-Jiménez, C.M., Castillo-Rodríguez, M., Molina-Aldareguia, J.M., Huang, Y. et al., "Controlling the High Temperature Mechanical Behavior of Al Alloys by Precipitation and Severe Straining," *Materials Science & Engineering A* 679(36-47), 2017, http://doi.org/10.1016/j.msea.2016.10.026.
15. Naghdy, S., Kestens, L., Hertelé, S., and Verleysen, P., "Evolution of Microstructure and Texture in Commercial Pure Aluminum Subjected to High Pressure Torsion Processing," *Materials Characterization* 120:285-294, 2016, http://doi.org/10.1016/j.matchar.2016.09.012.
16. Hohenwarter, A. and Wurster, S., "Deformation and Fracture Characteristics of Ultrafine-Grained Vanadium," *Materials Science & Engineering A* 650:492-496, 2016, http://doi.org/10.1016/j.msea.2015.10.052.
17. Estrin, Y. and Vinogradov, A., "Extreme Grain Refinement by Severe Plastic Deformation: A Wealth of Challenging Science," *Acta Materialia* 61(3):782-817, 2013, http://doi.org/10.1016/j.actamat.2012.10.038.
18. Sabbaghianrad, S. and Langdon, T.G., "Developing Superplasticity in an Aluminum Matrix Composite Processed by High-Pressure Torsion," *Materials Science & Engineering A* 655:36-43, 2016, http://doi.org/10.1016/j.msea.2015.12.078.
19. Han, J., Zhu, Z., Li, H., and Gao, C., "Microstructural Evolution, Mechanical Property and Thermal Stability of Al-Li 2198-T8 Alloy Processed by High Pressure Torsion," *Materials Science & Engineering A* 651:435-441, 2016, http://doi.org/10.1016/j.msea.2015.10.112.
20. Alhajeri, S.N., Al-Fadhalah, K.J., Almazrouee, A.I., and Langdon, T.G., "Microstructure and Microhardness of an Al-6061 Metal Matrix Composite Processed by High-Pressure Torsion," *Materials Characterization* 118:270-278, 2016, http://doi.org/10.1016/j.matchar.2016.06.003.
21. Zhilyaev, A.P. and Langdon, T.G., "Using High-Pressure Torsion for Metal Processing: Fundamentals and Applications," *Prog. Mater. Sci.* 53(6):893-979, 2008, http://doi.org/10.1016/j.pmatsci.2008.03.002.
22. Wongsa-Ngam, J., Kawasaki, M., Zhao, Y., and Langdon, T.G., "Microstructural Evolution and Mechanical Properties of a Cu-Zr Alloy Processed by High-Pressure Torsion," *Mater. Sci. Eng. A* 528(25-26):7715-7722, 2011, http://doi.org/10.1016/j.msea.2011.06.056.
23. Kawasaki, M., Alhajeri, S.N., Xu, C., and Langdon, T.G., "The Development of Hardness Homogeneity in Pure Aluminum and Aluminum Alloy Disks Processed by High-Pressure Torsion," *Mater. Sci. Eng. A* 529:345-351, 2011, doi:10.1016/j.msea.2011.09.039.

24. El-Garaihy, W.H., Ph.D. thesis, Production Engineering Department, Mansoura University, Mansoura, 2012, http://www.eulc.edu.eg/eulc_v5/Libraries/Thesis/BrowseThesisPages.aspx?fn=PublicDrawThesis&BibID=11842944.
25. Oraby, S.E., "Mathematical Modelling and In-Process Monitoring Techniques for Cutting Tools," PhD dissertation, University of Sheffield, Sheffield, 1989.
26. El-Garaihy, W.H., Rassoul, E.-S.M.A., and Salem, H.G., "Consolidation of High Performance AA6061 and AA6061-SiCp Composite Processed by High Pressure Torsion," *Materials Science Forum* 783-786:2623-2628, 2014, doi:10.4028/www.scientific.net/MSF.783-786.2623.
27. El-Garaihy, W.H., Alaskari, A.M., Ameshaiei, E.A., and Oraby, S.E., "On the Effect of HPT Processing Conditions on Relative Density, Mechanical Properties and Microstructural Evolution of Hot Compacted AA6061- Mathematical Empirical and Response Surface Approach," *Advanced Materials Letters* 8(5):620-628, 2016, doi:10.5185/amlett.2017.1402.
28. Langdon, T.G. and Xu, C., "Three-Dimensional Representations of Hardness Distributions after Processing by High-Pressure Torsion," *Mater. Sci. Eng. A* 503(1-2):71-74, 2009, http://doi.org/10.1016/j.msea.2008.04.083.
29. Stolyarov, V.V., Zhu, Y.T., Lowe, T.C., Islamgalive, R.K. et al., "Processing Nanocrystalline Ti and its Nanocomposites from Micrometer-Sized Ti Powder Using High Pressure Torsion," *Mater. Sci. Eng. A* 282:78-85, 2000, doi:10.1016/S0921-5093(99)00764-9.
30. Wei, X.S., Vekshin, B., Kraposhin, V., Huang, Y.J. et al., "Full Density Consolidation of Pure Aluminum Powders by Cold Hydro-Mechanical Pressing," *Mater. Sci. Eng. A* 528:5784-5789, 2011, http://doi.org/10.1016/j.msea.2011.03.099.
31. Wetscher, F., Vorhauer, A., and Pippan, R., "Strain Hardening during High Pressure Torsion Deformation," *Mater. Sci. Eng. A* 410-411:213-216, 2005, http://doi.org/10.1016/j.msea.2005.08.027.
32. Zhang, J., Gao, N., and Starink, M.J., "Al-Mg-Cu Based Alloys and Pure Al Processed by High Pressure Torsion: The Influence of Alloying Additions on Strengthening," *Mater. Sci. Eng.* A527(15):3472-3479, 2010, http://doi.org/10.1016/j.msea.2010.02.016.
33. Valiev, R.Z., Rovan, H.J., Liu, M., Murashkin, M. et al., "Nanostructures and Microhardness in Al and Al-Mg Alloys Subjected to SPD," *Materials Science Forum* 604-605:179-185, 2009, doi:MSF.604-605.179.
34. Chakrabarti, D.J. and Laughlin, D.E., "Phase Relations and Precipitation in Al-Mg-Si Alloys with Cu Additions," *Progress in Materials Science* 49(3-4):389-410, 2004, http://doi.org/10.1016/S0079-6425(03)00031-8.
35. Rajinikantha, V., Venkateswarlub, K., Sena, M.K., Dasa, M. et al., "Influence of Scandium on an Al-2% Si Alloy Processed by High-Pressure Torsion," *Mater. Sci. Eng. A* 528(3):1702-1706, 2011, http://doi.org/10.1016/j.msea.2010.10.102.
36. Langdon, T.G., Xu, C., and Horita, Z., "The Evolution of Homogeneity in an Aluminum Alloy Processed Using High-Pressure Torsion," *Acta Materialia* 56:5168-5176, 2008, http://doi.org/10.1016/j.actamat.2008.06.036.
37. Edalati, K., Daio, T., Horita, R.Z., Kishida, K. et al., "Evolution of Lattice Defects, Disordered/Ordered Phase Transformations and Mechanical Properties in Ni-Al-Ti Intermetallics by High-Pressure Torsion," *J. Alloys Compd.* 563:221-228, 2013, http://doi.org/10.1016/j.jallcom.2013.02.128.
38. Tian, Y.Z., Wu, S.D., Zhang, Z.F., Figueiredo, R.B. et al., "Microstructural Evolution and Mechanical Properties of a Two-Phase Cu-Ag Alloy Processed by High-Pressure Torsion to Ultrahigh Strains," *Acta Materialia* 59(7):2783-2796, 2011, http://doi.org/10.1016/j.actamat.2011.01.017.
39. Loucif, A., Figueiredo, R.B., Baudin, T., Brisset, F. et al., "Ultrafine Grains and the Hall-Petch Relationship in an Al-Mg-Si Alloy Processed by High-Pressure Torsion," *Mater. Sci. Eng. A* 532:139-145, 2012, http://doi.org/10.1016/j.msea.2011.10.074.
40. Liu, M., Rovan, H.J., Liu, X., Murashkin, M. et al., "Grain Refinement in Nanostructured Al-Mg Alloys Subjected to High Pressure Torsion," *J. Mater. Sci.* 45(17):4659-4666, 2010, doi:10.1007/s10853-010-4604-3.
41. Arsenault, R.J. and Shi, N., "Dislocation Generation due to Differences between the Coefficients of Thermal Expansion," *Mater. Sci. Eng.* 81:175-187, 1986, https://doi.org/10.1016/0025-5416(86)90261-2.